Nanoparticles

DOI: 10.1002/anie.201206703

# Bioorthogonal Copper-Free Click Chemistry In Vivo for Tumor-Targeted Delivery of Nanoparticles**

*Heebeom Koo, Sangmin Lee, Jin Hee Na, Sun Hwa Kim, Sei Kwang Hahn, Kuiwon Choi, Ick Chan Kwon, Seo Young Jeong, and Kwangmeyung Kim**

Nanoparticles have emerged as a promising tool in the biomedical field, in which they serve as delivery carriers of imaging agents or drugs for nanomedicines.[1] After intravenous injection, nanoparticles show higher accumulation in angiogenic disease sites than normal tissues as a result of the enhanced permeability and retention (EPR) effect.[2] To further improve their specificity to disease sites, active targeting strategies have been developed using biological targeting moieties, such as antibodies, aptamers, or peptides, which bind proper receptors on the surface of target cells.[3,4] Efficient binding of nanoparticles to the cell surface can increase their accumulation at the target site, while unbound nanoparticles are cleared from the tissue and eliminated from the body.[5] However, saturation of these receptors limits the capacity of targeted nanoparticles.[6] In addition, targetable receptors are rarely unique to the disease, so nanoparticles can accumulate in other healthy tissues through these receptors, resulting in reduced therapeutic efficacy and unintended side effects.[7] Furthermore, careful effort is needed to preserve the binding site and maintain the bioactivity of these targeting moieties during conjugation to nanoparticles.[8]

Currently, bioorthogonal chemistry with high specificity is paving the way for many novel innovations in the biological field.[9] Direct chemical reactions applicable in living systems with bioorthogonality and biocompatibility have garnered much attention from both chemists and biologists. For example, DNA, peptide, and protein can be modified by bioorthogonal chemistry in an easy and specific manner.[10] Recently, researchers have developed many chemicals for biocompatible copper-free click chemistry by focusing on ring-strained alkyne groups as the counterparts to azide groups for increased reactivity.[9b,11] With these chemical groups, various targeting moieties could be specifically conjugated to nanoparticles.[12] In particular, bioorthogonal chemistry has shown powerful applications in biological fields in combination with metabolic glycoengineering.[13] Through metabolic glycoengineering, unnatural glycans are introduced onto cells by feeding specific precursors on the basis of their intrinsic metabolism. Therefore, bioorthogonal chemical reactions can occur specifically on target living cells with artificially introduced unnatural glycans containing particular chemical groups, such as azides. Bertozzi's group pioneered this special technique and demonstrated it for various purposes, such as analysis of cellular glycan, 3D cellular assembly, exploiting metabolic pathways, and spatiotemporal imaging of zebrafish development.[14] However, there are only a few reports on applications to in vivo systems, especially for the targeted delivery of nanoparticles.[15] When applied in cancer nanomedicine, this bioorthogonal chemistry together with metabolic glycoengineering can greatly enhance the tumor-targetability of nanoparticles. This is because metabolic glycoengineering can artificially modulate the dose-dependent expression of unnatural targetable glycans in tumor tissue in vivo. Furthermore, we expect that bioorthogonal chemistry can be more effectively applied to nanoparticles than single molecules, because the multivalent effect (which is the enhanced binding by multiple targeting molecules) and the longer circulation time of nanoparticles can provide more chances and higher probability of binding to unnatural glycans on target cells in vivo.

Herein, we introduce a new in vivo active targeting strategy for nanoparticles through bioorthogonal copper-free click chemistry in the living body (Scheme 1). First, targetable glycans, unnatural sialic acids with azide groups, are artificially generated in target cancer cells by an intratumoral injection of the precursor, tetraacetylated N-azidoacetyl-D-mannosamine ($Ac_4ManNAz$).[15c] Second, nano-sized PEGylated liposomes (PEG = poly(ethylene glycol)) are modified with dibenzyl cyclootyne (DBCO) to strongly and specifically bind unnatural sialic acids by copper-free click chemistry.[16] Third, DBCO conjugated PEGylated liposomes (DBCO-lipo) are intravenously injected into tumor-bearing mice to chemically bind these unnatural sialic acids on the target cancer cell surface by in vivo bioorthogonal copper-free click chemistry. This technique is expected to enable dose-dependent and temporal generation of chemical groups on the target tumor site just like biological receptors, controlling the tumor-targetability of nanoparticles.

We selected $Ac_4ManNAz$ as the precursor for metabolic engineering of sialic acids, because $Ac_4ManNAz$ easily

[*] Dr. H. Koo,[+] Dr. S. H. Kim, Dr. K. Choi, Dr. I. C. Kwon, Dr. K. Kim
Center for Theragnosis, Biomedical Research Institute, Ko-rea Institute of Science and Technology
39-1 Hawolgok-dong, Seongbuk-gu, Seoul 136-791 (Korea)
E-mail: kim@kist.re.kr
S. Lee,[+] J. H. Na, Dr. S. Y. Jeong
Department of Life and Nanopharmaceutical Science
Kyung Hee University (Korea)
Dr. S. K. Hahn
Department of Materials Science and Engineering, Pohang University of Science and Technology (Korea)
[+] These authors contributed equally to this work.

[**] This study was funded by the Global Research Laboratory (GRL) Project, the Fusion Technology Project (2009-0081876), and the Intramural Research Program (Theragnosis) of KIST.
Supporting information for this article is available on the WWW under http://dx.doi.org/10.1002/anie.201206703.

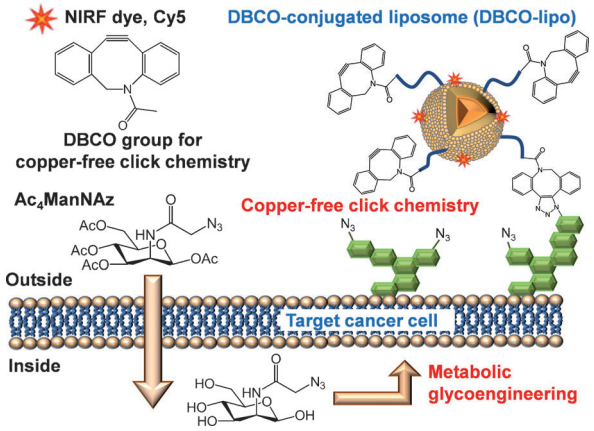


***Scheme 1.*** Schematic illustration of in vivo tumor-targeting strategy for nanoparticles by bioorthogonal copper-free click chemistry; see text for details.

produces the unnatural sialic acids on tumor cell surface.[17] As expected, $Ac_4$ManNAz-treated A549 human lung cancer cells successfully produced unnatural and targetable sialic acids on their surface in a dose-dependent manner. Generated azide groups on the cell surface were visualized in green fluorescence after treatment of A549 tumor cells with phosphine-FLAG and FLAG-FITC (Figure 1a). Furthermore, coomassie blue staining and western blot analysis of $Ac_4$ManNAz-treated cells showed the $Ac_4$ManNAz dose-dependent expression of unnatural targetable sialic acids (Figure 1b). This dose-dependent expression of unnatural targetable sialic acids on the target tumor cells is very unique compared to other natural targeting moieties such as receptors for RGD, folate, or other antibodies.

To target unnatural sialic acids with azide groups, DBCO was chosen as a bioorthogonal chemical group because of its high reactivity to azide groups through copper-free click reactions.[16] PEGylated liposomes, as a conventional nanoparticle delivery system, were modified with DBCO (Figure 1c). Briefly, activated DBCO (sulfo-DBCO-NHS) was conjugated to amine-functionalized PEG-lipids and incorporated into liposomes during their fabrication by a traditional film-casting method, resulting in DBCO-lipo (see Figure S1, S2, and S3 in the Supporting Information). A 10 mol% of DBCO-modified PEG-lipids per total lipid composition was incorporated into DBCO-lipo, while PEGylated liposomes without DBCO (PEG-lipo) were used as a control. For in vitro and in vivo near-infrared fluorescence (NIRF) tracking of liposomes, 0.5 molar ratio of Cy5-labeled lipids were incorporated into DBCO-lipo and PEG-lipo. As expected, the resulting liposomes had a stable spherical shape as shown in CryoTEM images, and the size of DBCO-lipo was $75.33 \pm 18.29$ nm in aqueous condition as determined by dynamic light scattering (DLS; Figure 1d and Figure S4 in the Supporting Information). In addition, after incubation in 10% FBS containing media, the size distribution of DBCO-lipo slightly increased to $110.79 \pm 21.35$ nm. However, these nanoparticles were still small enough to freely move in blood flow and showed no further aggregation.

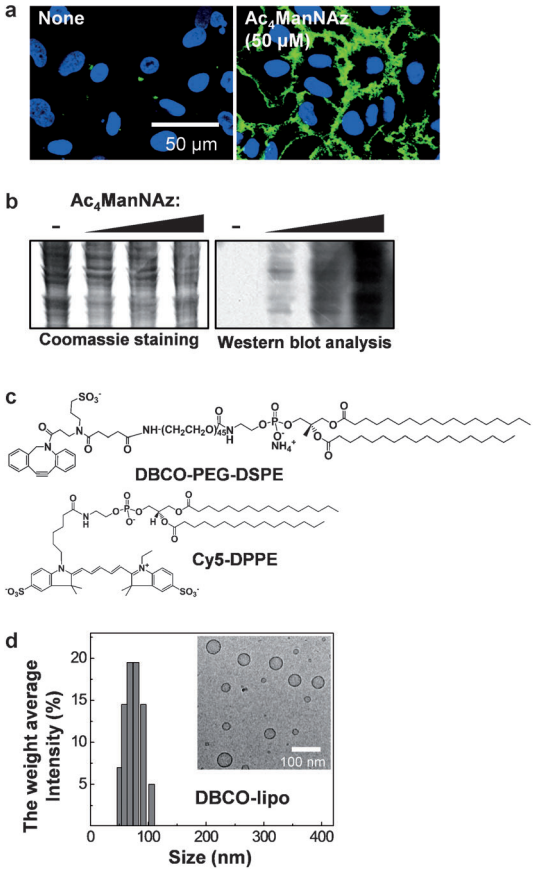


***Figure 1.*** Introduction of unnatural sialic acids with azide groups on the cell surface and preparation of DBCO-functionalized liposomes (DBCO-lipo). a) Visualization of azide groups (green) on the surface of $Ac_4$ManNAz-treated A549 cells. b) Coomassie staining and western blot analysis of $Ac_4$ManNAz-treated cells (dose increases from left to right) showing the amount of total proteins and generated azide groups, respectively. c) Chemical structures of DBCO-PEG-DSPE and Cy5-labeled DPPE. d) The morphology (TEM image) and size distribution of DBCO-lipo (determined by DLS).

In this $Ac_4$ManNAz-treated cell culture system, the binding of DBCO-lipo to the A549 tumor cells was visualized by Cy5 fluorescence. The amount of bound DBCO-lipo on the cell surface increased along with the increasing number of azide groups, indicating the high reactivity of copper-free click approach (Figure 2a). This result indicates that the binding of nanoparticles can be artificially controlled by changing the concentration of $Ac_4$ManNAz in a dose-dependent manner. As a control, PEG-lipo without DBCO showed minimal binding to the $Ac_4$ManNAz-treated tumor cells (Figure 2b). Also, after treatment with tris(2-carboxyethyl)-phosphine (TCEP) to chemically quench azide groups, the binding efficiency of DBCO-lipo dramatically decreased showing the high specificity of DBCO-lipo and azide groups.[14d] DBCO conjugated with Cy5 (DBCO-Cy5) was used as a control. Interestingly, the fluorescence intensity of DBCO-Cy5-treated tumor cells was even lower than that of DBCO-lipo treated cells. The greatly increased binding of DBCO-lipo, compared to DBCO-Cy5 at the same molar concentration of NIRF dye, might be ascribed to the multi-

  

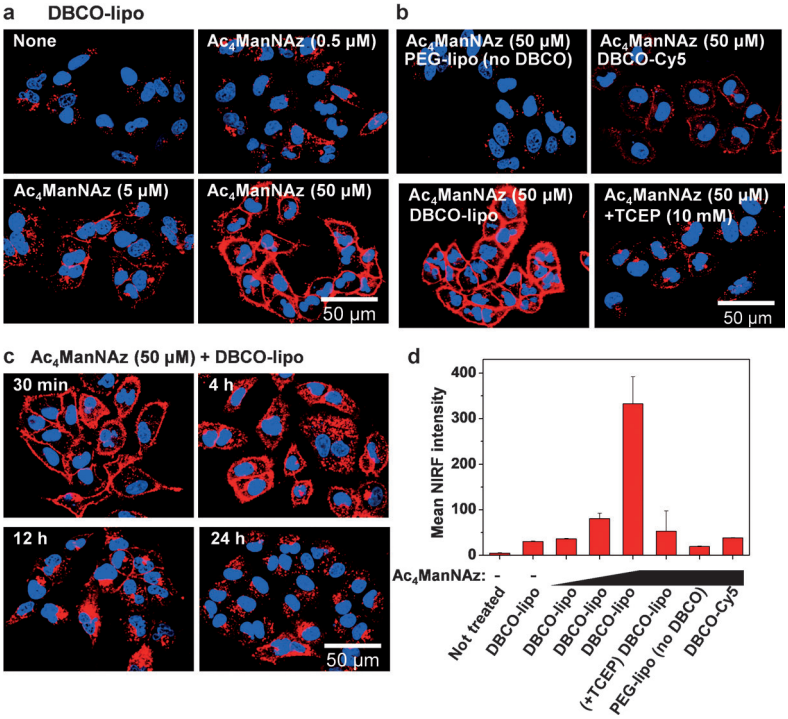


***Figure 2.*** Cellular binding and uptake of DBCO-lipo. a) $Ac_4ManNAz$ concentration-dependent binding of DBCO-lipo (red) to A549 cells (blue). b) Binding of DBCO-lipo to $Ac_4ManNAz$-treated cells and control experiments with other groups, see text for details. c) Time-lapse images of DBCO-lipo (red) in $Ac_4ManNAz$-treated cells. d) Flow cytometry data of $Ac_4ManNAz$-treated cells after binding with DBCO-lipo (see text for details).

valent effect of nanoparticles in accordance with previous reports on RGDs or folates on the nanoparticle surface.[18] There was a ratio of about one Cy5 dye molecule to 20 DBCO groups in our DBCO-lipo and the binding efficiency was dependent on the amount of DBCO (see Figure S5 in the Supporting Information). Importantly, DBCO-lipo exhibited the similarly higher tumor-targeting ability in different $Ac_4ManNAz$-treated-tumor cells (U87MG, MCF-7, and KB cells, see Figure S6 in the Supporting Information), regardless of the heterogeneity of different tumor cell lines. This result suggests that this higher tumor-targeting efficiency of DBCO-lipo in $Ac_4ManNAz$-treated cell culture system is mainly caused by the bioorthogonal copper-free click chemistry.

In addition, we investigated the intracellular fate of these nanoparticles that are chemically bound to the cell surface, which is important for their further application as drug carriers. The bound DBCO-lipo was taken up by cells as shown in time-lapse imaging (Figure 2c). It may be due to the intrinsic glycan internalization followed by endocytosis of nanoparticles, which is significant for the intracellular delivery of drugs.[15b] In the flow cytometry data, the fluorescence intensity of 50 μM $Ac_4ManNAz$-treated cells was more than 20-fold higher than that of control tumor cells without $Ac_4ManNAz$ treatment (Figure 2d). The 5 μM $Ac_4ManNAz$-treated cells showed about 2.6-fold increased fluorescence over the control, while the change was negligible in the case of 0.5 μM $Ac_4ManNAz$. Furthermore, the intensity of DBCO-lipo in 50 μM $Ac_4ManNAz$-treated cells was about 13.8- and 6.8-fold higher than the case of PEG-lipo and TCEP treatment, respectively, indicating the high specificity of the copper-free click chemistry.

For in vivo studies, we prepared xenograft mice models bearing two tumors in both sides of the flank by subcutaneous injection of A549 tumor cells. Then, different concentrations of $Ac_4ManNAz$ were administered to the left tumors by intratumoral injection for three days while saline was injected to the right as a control. The Coomassie blue staining and western blot analysis of tumor tissues showed that the amount of unnatural sialic acid with azide groups increased in a dose-dependent manner similarly with the cellular conditions (Figure 3a). Histological staining using phosphine-FLAG and FLAG-HRP also visualized the dose-dependent generation of azide groups only in $Ac_4ManNAz$-treated tumors (Figure 3b and see Figure S7 and S8 in the Supporting Information). The opposite tumor tissue of the same mice showed negligible generation of azide groups compared to the 50 mM $Ac_4ManNAz$-treated tumors. These results indicate that metabolic glycoengineering can artificially modulate the expression of unnatural targetable sialic acids in a dose-dependent manner even under in vivo conditions.

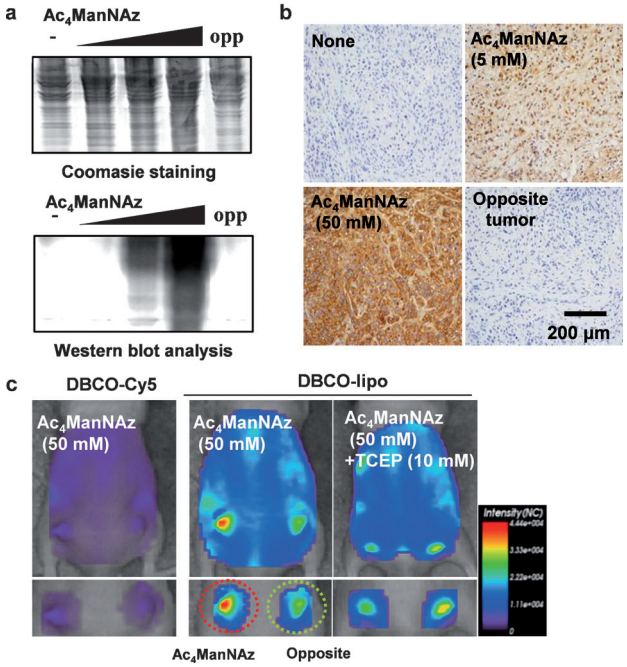


***Figure 3.*** In vivo tumor-targeting of DBCO-lipo in tumor-bearing mice models. a) Coomassie staining and western blot analysis of $Ac_4ManNAz$-treated tumor tissues; opp = opposite (control) tumor. b) Histological staining of $Ac_4ManNAz$-treated tumor tissues using phosphine-FLAG and FLAG-HRP. c) Whole body biodistribution of DBCO-lipo in $Ac_4ManNAz$-treated tumor-bearing mice. (left: $Ac_4ManNAz$-treated, right: saline-treated).

When the tumor diameters grew to 10 mm, they were treated with $Ac_4$ManNAz in the same way for three days, and 10 mg kg$^{-1}$ of DBCO-lipo and PEG-lipo were intravenously injected to these mice. Also, the control DBCO-Cy5 was injected into mice with the same NIRF intensity as that of liposome solutions. Whole body distribution and tumor-targetabilty of each sample were quantified using a non-invasive optical imaging system in live animals. As expected, PEG-lipo showed no difference in fluorescence intensity in tumors with or without $Ac_4$ManNAz (see Figure S9 in the Supporting Information). It showed slightly higher accumulation in tumor tissue than normal surrounding tissue only because of the EPR effect of nano-sized carriers. Also, it showed the nonspecific binding to normal organs, such as liver and kidney.[19] However, the amount of accumulated DBCO-lipo highly increased in the $Ac_4$ManNAz-treated left-side tumors compared to the saline-treated right-side tumors after intravenous injection of DBCO-lipo. The increased accumulation of DBCO-lipo was higher in 50 mM $Ac_4$ManNAz-treated tumors than the case of 5 or 0.5 mM, showing that the binding of DBCO-lipo was also dependent on the concentration of $Ac_4$ManNAz as tested under in vitro conditions. This artificial tumor-targeting of nanoparticles in a dose-dependent manner is the unique advantage of the targeting strategy based on metabolic glycoengineering and bioorthogonal chemistry over other active targeting strategies with biological targeting moieties. The similar intensities in both tumors after TCEP treatment strongly suggested that the increased DBCO-lipo accumulation was based on the copper-free click chemistry. Interestingly, DBCO-Cy5-treated mice gave relatively dim images, which may be due to the short circulation time of DBCO-Cy5 and its lack of the multivalent effect. The result reveals that this technique is more suitable for nanoparticles than small molecules.

Finally, ex vivo tumor tissue analysis confirmed the significant tumor-targeting of DBCO-lipo by the bioorthogonal copper-free click chemistry in vivo. Five hours post-injection, tumors and other organs were dissected, and each sample was analyzed in a Kodak imaging box. NIRF images of tumor groups also confirmed that the amount of accumulated DBCO-lipo significantly increased according to the concentration of treated $Ac_4$ManNAz (Figure 4a). This result showed that the biodistribution of nanoparticles could be artificially controlled using chemical precursors in a dose-dependent manner. In the case of 50 mM $Ac_4$ManNAz-treated tumors, the amount of DBCO-lipo increased almost twofold higher than saline-treated tumors on the opposite side of the mouse (Figure 4b). On the other hand, the accumulation of control DBCO-Cy5 in tumor tissue was significantly lower than DBCO-lipo, and the difference between the tumors was hardly observed owing to their short blood circulation and fast excretion from the body. The NIRF intensity of DBCO-Cy5 was only about 5.6% of DBCO-lipo in 50 mM $Ac_4$ManNAz-treated tumors. These data support that the long circulation and the multivalent effect of nanoparticles are helpful for bioorthogonal copper-free click chemistry especially under in vivo conditions. The brown color in histological staining and the intense red spots of DBCO-lipo in $Ac_4$ManNAz-treated tumor tissues indicated the correlation of the generated azide groups and the amount of accumulated DBCO-lipo (Figure 4c). These results confirmed that nanoparticles could be delivered to the target site by in vivo copper-free click chemistry reaction with bioorthogonal chemical groups in artificially introduced unnatural sialic acids.

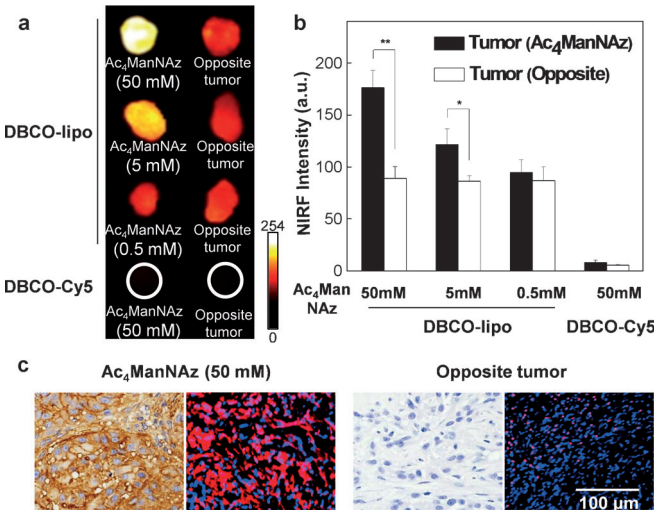


***Figure 4.*** Ex vivo tumor tissue analysis of tumor-bearing mice models after intravenous injection of DBCO-lipo. a) NIRF images of tumor groups from $Ac_4$ManNAz-treated tumor-bearing mice after intravenous injection of DBCO-lipo. b) The mean NIRF intensities of samples in (a). c) Histological staining and fluorescence images of $Ac_4$ManNAz-treated tumor tissues after intravenous injection of DBCO-lipo. Symbols * and ** indicate differences at the $p < 0.05$ and $< 0.01$ significant levels, respectively (analyzed using one-way ANOVA).

In summary, the overall results successfully demonstrated the potential of this new in vivo targeting strategy of nanoparticles based on bioorthogonal copper-free click chemistry. Unnatural sialic acids with azide groups could be artificially generated on the target site by metabolic glycoengineering. Then, these groups could effectively enhance the accumulation of nanoparticles in the target site through bioorthogonal copper-free click chemistry inside the living body. Importantly, after binding the cell surface, these nanoparticles were taken up into the cells over time showing the feasibility for targeted intracellular drug delivery. The efficiency of this technique can be improved with the development of new bioorthogonal chemical groups with higher reactivity. Taken together, this technique will be highly useful for the targeted delivery of nanoparticles for imaging and drug delivery.

Received: August 18, 2012
Published online: October 19, 2012

**Keywords:** click chemistry · drug delivery · metabolic glycoengineering · nanoparticle · tumor targeting

[1] R. A. Petros, J. M. DeSimone, *Nat. Rev. Drug Discovery* **2010**, *9*, 615–627.
[2] V. Torchilin, *Adv. Drug Delivery Rev.* **2011**, *63*, 131–135.

  

[3] a) J. D. Byrne, T. Betancourt, L. Brannon-Peppas, *Adv. Drug Delivery Rev.* **2008**, *60*, 1615 – 1626; b) H. Koo, M. S. Huh, I.-C. Sun, S. H. Yuk, K. Choi, K. Kim, I. C. Kwon, *Acc. Chem. Res.* **2011**, *44*, 1018 – 1028.
[4] O. C. Farokhzad, J. M. Karp, R. Langer, *Expert Opin. Drug Delivery* **2006**, *3*, 311 – 324.
[5] H. S. Choi, W. Liu, F. Liu, K. Nasr, P. Misra, M. G. Bawendi, J. V. Frangioni, *Nat. Nanotechnol.* **2010**, *5*, 42 – 47.
[6] J. W. Park, K. Hong, D. B. Kirpotin, G. Colbern, R. Shalaby, J. Baselga, Y. Shao, U. B. Nielsen, J. D. Marks, D. Moore, D. Papahadjopoulos, C. C. Benz, *Clin. Cancer Res.* **2002**, *8*, 1172 – 1181.
[7] S. M. Moghimi, A. C. Hunter, J. C. Murray, *Pharmacol. Rev.* **2001**, *53*, 283 – 318.
[8] S. Bhattacharyya, R. D. Singh, R. Pagano, J. D. Robertson, R. Bhattacharya, P. Mukherjee, *Angew. Chem.* **2012**, *124*, 1595 – 1599; *Angew. Chem. Int. Ed.* **2012**, *51*, 1563 – 1567.
[9] a) M. Boyce, C. R. Bertozzi, *Nat. Methods* **2011**, *8*, 638 – 642; b) E. M. Sletten, C. R. Bertozzi, *Acc. Chem. Res.* **2011**, *44*, 666 – 676.
[10] a) T. Plass, S. Milles, C. Koehler, C. Schultz, E. A. Lemke, *Angew. Chem.* **2011**, *123*, 3964 – 3967; *Angew. Chem. Int. Ed.* **2011**, *50*, 3878 – 3881; b) J. L. Seitchik, J. C. Peeler, M. T. Taylor, M. L. Blackman, T. W. Rhoads, R. B. Cooley, C. Refakis, J. M. Fox, R. A. Mehl, *J. Am. Chem. Soc.* **2012**, *134*, 2898 – 2901; c) I. S. Carrico, B. L. Carlson, C. R. Bertozzi, *Nat. Chem. Biol.* **2007**, *3*, 321 – 322; d) N. K. Devaraj, R. Weissleder, *Acc. Chem. Res.* **2011**, *44*, 816 – 827.
[11] C. R. Bertozzi, *Acc. Chem. Res.* **2011**, *44*, 651 – 653.
[12] M. Colombo, S. Sommaruga, S. Mazzucchelli, L. Polito, P. Verderio, P. Galeffi, F. Corsi, P. Tortora, D. Prosperi, *Angew. Chem.* **2012**, *124*, 511 – 514; *Angew. Chem. Int. Ed.* **2012**, *51*, 496 – 499.
[13] K. J. Yarema, S. Goon, C. R. Bertozzi, *Nat. Biotechnol.* **2001**, *19*, 553 – 558.
[14] a) J. A. Prescher, C. R. Bertozzi, *Cell* **2006**, *126*, 851 – 854; b) Z. J. Gartner, C. R. Bertozzi, *Proc. Natl. Acad. Sci. USA* **2009**, *106*, 4606 – 4610; c) M. Boyce, I. S. Carrico, A. S. Ganguli, S.-H. Yu, M. J. Hangauer, S. C. Hubbard, J. J. Kohler, C. R. Bertozzi, *Proc. Natl. Acad. Sci. USA* **2011**, *108*, 3141 – 3146; d) S. T. Laughlin, J. M. Baskin, S. L. Amacher, C. R. Bertozzi, *Science* **2008**, *320*, 664 – 667.
[15] a) J. A. Prescher, D. H. Dube, C. R. Bertozzi, *Nature* **2004**, *430*, 873 – 877; b) J. M. Baskin, J. A. Prescher, S. T. Laughlin, N. J. Agard, P. V. Chang, I. A. Miller, A. Lo, J. A. Codelli, C. R. Bertozzi, *Proc. Natl. Acad. Sci. USA* **2007**, *104*, 16793 – 16797; c) P. V. Chang, J. A. Prescher, E. M. Sletten, J. M. Baskin, I. A. Miller, N. J. Agard, A. Lo, C. R. Bertozzi, *Proc. Natl. Acad. Sci. USA* **2010**, *107*, 1821 – 1826.
[16] X. Ning, J. Guo, M. A. Wolfert, G.-J. Boons, *Angew. Chem.* **2008**, *120*, 2285 – 2287; *Angew. Chem. Int. Ed.* **2008**, *47*, 2253 – 2255.
[17] a) J. A. Prescher, C. R. Bertozzi, *Nat. Chem. Biol.* **2005**, *1*, 13 – 21; b) A. Matsumoto, H. Cabral, N. Sato, K. Kataoka, Y. Miyahara, *Angew. Chem.* **2010**, *122*, 5626 – 5629; *Angew. Chem. Int. Ed.* **2010**, *49*, 5494 – 5497.
[18] a) X. Montet, M. Funovics, K. Montet-Abou, R. Weissleder, L. Josephson, *J. Med. Chem.* **2006**, *49*, 6087 – 6093; b) S. Hong, P. R. Leroueil, I. J. Majoros, B. G. Orr, J. R. Baker, Jr., M. M. Banaszak Holl, *Chem. Biol.* **2007**, *14*, 107 – 115.
[19] H. S. Choi, K. Nasr, S. Alyabyev, D. Feith, J. H. Lee, S. H. Kim, Y. Ashitate, H. Hyun, G. Patonay, L. Strekowski, M. Henary, J. V. Frangioni, *Angew. Chem.* **2011**, *123*, 6382 – 6387; *Angew. Chem. Int. Ed.* **2011**, *50*, 6258 – 6263.

  